Electrolysis of pyrolysis oil distillates and permeates in a multi-anode proton exchange membrane cell

Tobias M. Brueckner[a], Kelly A. Hawboldt[a], Peter G. Pickup[b],*

[a] Department of Process Engineering, Faculty of Engineering and Applied Sciences, Memorial University of Newfoundland, St. John's, NL, A1B 3X5, Canada
[b] Department of Chemistry, Memorial University of Newfoundland, St. John's, NL, A1B 3X7, Canada

ARTICLE INFO

## ABSTRACT

Pyrolysis oil from softwood forestry residues (sawdust and bark) often contains too much water to be a useful fuel. Excess water can be removed by distillation or pervaporation to meet the ASTM burner fuel standard, while producing methanol rich aqueous distillates/permeates. This work focuses on electrolysis of the aqueous by-product stream to produce hydrogen. Short-path vacuum distillation produced the best fuel, but acetic acid, hydroxyacetone, acrolein, and other impurities strongly suppressed the electrolysis of the methanol. However, fractional distillation produced a distillate that could be electrolyzed at 14 mA cm^{-2} at 0.4 V at a PtRu catalyst, and 220 mA cm^{-2} at 0.9 V at a Pt catalyst. Pervaporation also produced a standard fuel, while electrolysis of permeates produced current densities as high as 44 mA cm^{-2} at 0.5 V and 240 mA cm^{-2} at 0.9 V. There is scope for substantial improvements by decreasing the effect of impurities.

1. Introduction

Electrolysis of water to produce hydrogen for fuel cells is one of the leading technologies for storing renewable energy and for sustainable power production [1–3]. However, there are significant challenges and inefficiencies in current systems [2], and innovative approaches are being taken to develop alternative electrolysis technologies [4]. The high theoretical potential difference required for water electrolysis to produce H_2 and O_2, together with the high overpotential for O_2 evolution, and the low economic value of O_2, have prompted growing research into the use of alternative anode reactions [4–9]. For example, oxidation of methanol at the anode (Eq. (1)) allows hydrogen to be produced at the cathode (Eq. (2)) at much lower potentials than the ca. 1.5 V required for electrolysis of water [10].

$$CH_3OH + H_2O \rightarrow CO_2 + 6H^+ + 6e^- \qquad (1)$$

$$6H^+ + 6e^- \rightarrow 3H_2 \qquad (2)$$
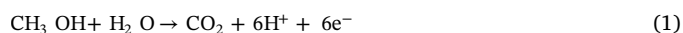
Although electrolysis of methanol [10], ethanol [11], or formic acid [12] solutions greatly decreases the potential difference and energy required to produce H_2, these are valuable commodities. Consequently, electrolysis of various types of crude biomass and low value byproducts has become of major interest [4,13–19]. Generally, microbial electrolysis cells have been used to facilitate the breakdown and oxidation of complex biological materials [14], although chemical degradation and

direct oxidation can be used at elevated temperatures [16,17]. A major attraction of technologies based on the electrolysis of materials derived from biomass is that the products can be used for other applications and often have added value [4,18,20–22].

The purpose of the work reported here was to investigate the electrolysis of aqueous distillates and permeates produced from pyrolysis oils derived from softwood forestry residues (sawdust and bark). Low temperature distillation or pervaporation of water and acetic acid from the pyrolysis oil improves the heating value, while producing a distillate or permeate containing value-added chemicals such as acetic acid, methanol, formic acid, and hydroxyacetone (acetol) [23]. Since methanol and formic acid can easily be electrolyzed to produce H_2 and CO_2, it was envisaged that the value of the "waste" stream from enhancing oil quality could be increased in this way (Fig. 1). Following capture of H_2 and CO_2 from the cell exhaust, the major components would be acetic acid and hydroxyacetone, which could be easily separated.

2. Experimental

2.1. Materials

Methanol (99.8%; ACP Chemical Inc.), acetic acid (Caledon Laboratory Chemicals), hydroxyacetone (90% containing ≤500 ppm

---

* Corresponding author.
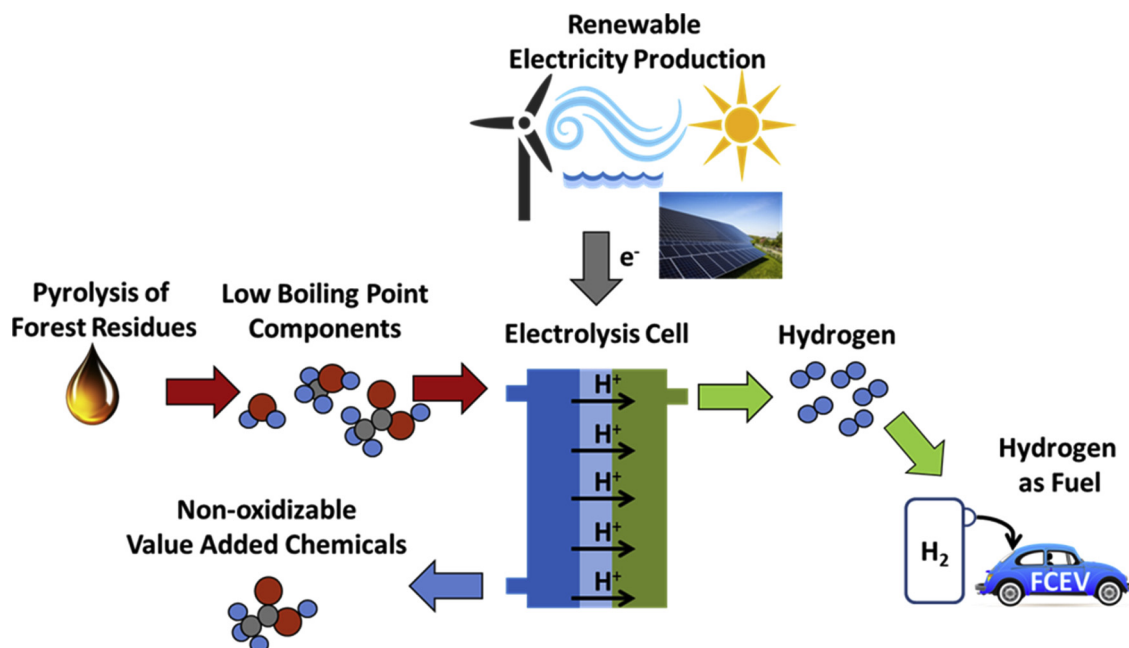 *E-mail address:* ppickup@mun.ca (P.G. Pickup).

Fig. 1. Flow chart for production of hydrogen and value-added chemicals from distillates and permeates produced during removal of water from pyrolysis oil.

sodium carbonate as stabilizer; Sigma-Aldrich Co.), acrolein (90% containing hydroquinone as stabilizer; Sigma-Aldrich Co.), were used as received. Distilled, filtered deionized water and industrial grade nitrogen (NI-K, 99.998%; Air Liquide) were used in all electrolysis experiments. Nafion 115 and 117 membranes (DuPont) were cleaned at 80 °C in 3% H_2O_2 (aq) (EMD Millipore) and 1 M H_2SO_4 (aq) (Fisher Scientific), rinsed with deionized water, and stored in deionized water. Anodes consisted of the following catalysts on Toray carbon paper: platinum black (Pt; 4.0 mg cm^{-2}); platinum-ruthenium black (PtRu; 1:1 atomic ratio; Johnson Matthey; 5.4 mg cm^{-2}); carbon supported Pt (Pt/C; 4.0 mg cm^{-2}; HiSPEC 13100, 70% Pt by mass on a high surface area advanced carbon support; Alfa Aesar); carbon-supported PtRu (PtRu/C; 4.0 mg PtRu cm^{-2}; HiSPEC 12100, 50% Pt and 25% Ru by mass on a high surface area advanced carbon support; Alfa Aesar). The Pt black electrodes contained polytetrafluoroethylene as a binder, while the PtRu black anodes contained 15 mass% Nafion and the anodes prepared with supported catalysts contained 20% Nafion. The preparation of the electrodes is described in [24].

2.2. Pyrolysis oils

Two different pyrolysis oils were used in this study. They were produced from small-scale (40 kg day^{-1}) and large-scale (1 t day^{-1}) versions of the same ABRITech auger reactor at 475 °C with steel shot as a heat carrier, as described in [25]. Softwood shavings (sourced from the Sexton Sawmill in Newfoundland) were processed in the 40 kg day^{-1} unit, while bark oil (spruce, pine, and fir softwood bark sourced from Groupe Crête division St-Faustin Inc. sawmill in Mont-Tremblant, Quebec, Canada) was produced at ABRITech's facility in the 1 t day^{-1} plant in Namur, Quebec. Several different batches of each oil were used. The softwood pyrolysis oil consisted of a single phase and has been characterized in [23]. The bark pyrolysis oil formed two phases, an aqueous top and a heavy bottom phase. Only the aqueous phase of bark pyrolysis oil was used in this work.

The water contents of the crude and upgraded oils were determined according to ASTM E203 as recommended in ASTM D7544 12 with a Mettler Toledo C20 Compact Karl Fischer Coulometer. Higher heating values (HHV) were measured according to ASTM D240 with a Parr B41 calorimeter with a 1108 oxygen combustion bomb and a model 6775 digital thermometer.

2.3. Distillation, pervaporation, and analysis

A small-scale (25 g) short-path vacuum distillation described in [23] was used initially for separation of water and volatile components from the softwood oil. Distillation of a 25 g aliquot of oil at 80 °C and 10 kPa for 1 h produced ca. 5 g of aqueous distillate [23].

Fractional distillation of the aqueous phase of bark pyrolysis oil (250 mL) was conducted at ambient pressure with a 500 mL distillation flask and 50 cm Vigreux fractionation column. The temperatures in both the boiling liquid and the distillation head remained constant at 100 °C ± 2 °C during collection of all fractions, due to the large percentage of water (ca. 60–70 mass%).

Separation of water and volatile components from the aqueous phase of bark pyrolysis oil by pervaporation was carried out with Nafion™ 211 (Dupont) and Pervap™ 4155-30 and 4101 (DeltaMem AG) membranes. The Pervap membranes have a 0.5–5 μm thick polyvinyl alcohol (PVA) separation layer on a porous 70–100 μm thick polyacrylonitrile porous support layer on a 100–150 μm thick porous polyester mechanical support layer. The PVA separation layer of Pervap 4155-30 is less crosslinked than that of Pervap 4101. The membrane was sandwiched between two stainless steel plates with serpentine flow fields consisting of three parallel flow channels (1.6 mm wide and 1.0 mm deep). The membrane area was 12 cm^2 for Nafion and 56 cm^2 for the Pervap membranes. The unit was heated to 80 °C (60 °C for the Nafion membrane). Bark oil (50 mL, or 20 mL for Nafion) was pumped through one flow field at 0.1 mL min^{-1} with a NE-300 New Era Pump Systems syringe pump, while nitrogen was passed through the other flow field at 10 mL min^{-1} to collect the permeate. The permeate vapours were condensed in a trap cooled with an ice + dry ice mixture. A partial vacuum (20 kPa) was applied for the Pervap membranes, to increase the permeation rate.

Distillates and permeates were stored at approximately 5 °C prior to analysis. They were analyzed by proton nuclear magnetic resonance (NMR) spectroscopy with a Bruker AVANCE III 300 MHz NMR spectrophotometer, following the addition of D_2O (60% by volume), and fumaric acid as an internal standard. This method provides accurate analysis of the identified components with a precision of ca. ± 1% [26].
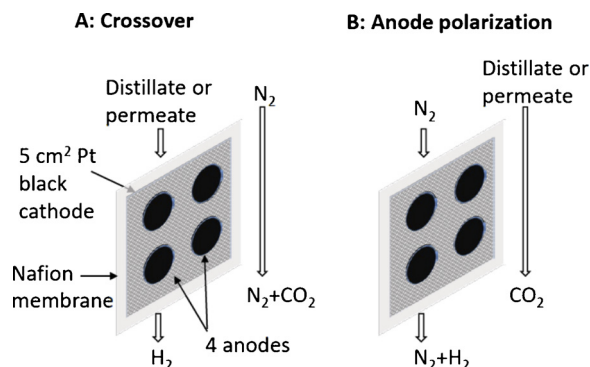
Fig. 2. Schematic diagrams of the membrane and electrode assembly for the 4-anode electrolysis cell, showing the crossover (A) and anode polarization (B) modes of operation.

2.4. Electrolysis of distillates and permeates

Electrolysis was carried out at 80 °C in multi-anode proton exchange membrane (PEM) cells based on a modified commercial (ElectroChem Inc.) PEM fuel cell [24]. A 5 cm^2 Pt black cathode, a Nafion™ proton conducting membrane, and four (0.385 cm^2) or nine (0.236 cm^2) separate anodes were sandwiched between the commercial cathode graphite flow field plate and a Lexan or Bakelite plate with a similar flow field, containing graphite rods as the anode current collectors [24]. The applied potential was controlled with a MSTAT multi-channel potentiostat from Arbin Instruments. The aqueous fuel solution was supplied at 0.5 mL min^{-1} by a NE-300 New Era Pump Systems syringe pump.

In initial experiments (Sections 3.1 and 3.2), a four-anode cell with a Nafion 115 membrane was operated in crossover mode (Fig. 2A), with the liquid fuel solution pumped through the cathode flow field while the anode flow field was purged with nitrogen at 10 mL min^{-1}. Two Pt black and two PtRu black anodes were used in order to monitor reproducibility. In later experiments (Sections 3.3 and 3.4), a nine-anode cell with a Nafion 117 membrane was operated in anode polarization mode (Fig. 2B) with three Pt/C anodes, three PtRu/C anodes and three anodes prepared by mixing the Pt/C and PtRu/C catalysts in a 1:1 mass ratio. The liquid fuel solution was pumped through the anode flow field while the cathode flow field was purged with nitrogen. Hydrogen was produced at the cathode (Eq. (2)) in both modes of operation of the cell. Although the fuel solution passes sequentially from one anode to the next in these cells, reproducibility between anodes is good (± 7% [24]) and there are no significant effects due to products from other anodes.

Prior to each experiment, the cell was preconditioned with 1 M aqueous methanol at 0.7 V for 1 h at 80 °C. Then polarization curves were obtained for the test solution (distillate, permeate or artificial mixture) from 0.9 V to 0.0 V in 25 or 50 mV steps. Each potential was held for three minutes, with the current recorded every second. The reported currents are averages over the final two minutes.

Each cell, with the same membrane and electrode assembly, was used over a period of several months. Between measurements, it was washed thoroughly by flushing the anode flow field with water at 80 °C for 2–4 h. Prior to any measurements with distillates, permeates, or methanol solutions containing added impurities, a polarization curve was obtained with 1 M methanol to confirm that the performance had not been significantly degraded.

3. Results and discussion

3.1. Composition, purification, and electrolysis of a sample from short-path vacuum distillation of softwood oil

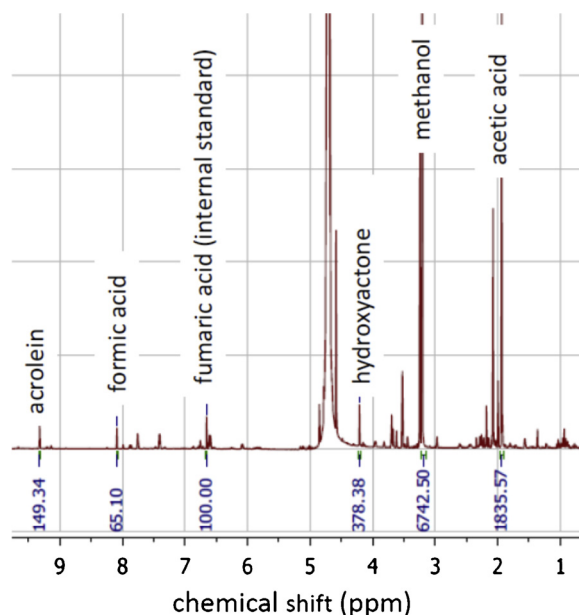Initially, use of the aqueous distillate obtained by short-path

Fig. 3. Proton NMR spectrum of the softwood oil distillate that was oxidized in the 4-anode cell.

vacuum distillation of softwood pyrolysis oil at 80 °C, reported in [23], was explored. A 30 mL sample was produced by repeating the small batch scale distillation a number of times. NMR spectroscopy showed that it contained 0.53 M methanol, 0.88 M acetic acid, 0.40 M hydroxyacetone, 0.03 M formic acid, and 0.03 M prop-2-enal (acrolein), with a large number of minor components such as furfural, 2-furfuryl alcohol and 2-acetylfuran [23]. Characterization of the residual, enhanced oil from this process has been previously reported [23]. The water content of the original bio-oil could be decreased by 55% (from 33.7 to 14.9 mass%) with an increase in the higher heating value (HHV) from 13.6 to 21.3 kJ g^{-1}, and decrease in the total acid number from 85.2 to 63.5 mg g^{-1}. The original oil did not meet the ASTM D7544-12 standard for a burner fuel, of water ≤ 30% and HHV ≥ 15 kJ g^{-1}, while the enhanced oil significantly exceeded the standard.

To concentrate the methanol, and decrease the acetic acid concentration in the distillate from the vacuum distillation, a conventional laboratory scale fractional distillation was performed, and the 1st fraction (6 mL) was tested in a 4-anode electrolysis cell. An NMR spectrum of this sample is shown in Fig. 3. Peaks for methanol (2.02 M), acetic acid (0.55 M), hydroxyacetone (0.17 M), acrolein (0.13 M), and formic acid (0.06 M) are identified.

Polarization curves (Fig. 4) for electrolysis of this fraction were recorded simultaneously at two Pt black electrodes and two PtRu black electrodes to check reproducibility, and assess the significance of differences between the two catalysts. PtRu is the preferred catalyst for the electrochemical oxidation of methanol because surface Ru−OH groups promote the oxidation of the adsorbed CO intermediate (Pt-CO) at lower potentials than on a pure Pt surface [27,28]. This follows a Langmuir–Hinshelwood mechanism and is often referred to as a bifunctional effect. At elevated temperatures, methanol can also be oxidized directly on the Ru sites, although this is much slower than the bifunctional mechanism on a 1:1 atomic ratio PtRu alloy [29]. Pt electrodes were also used in this study because the impurities in the pyrolysis oil distillates and permeates would be expected to adsorb differently on the two catalysts, and the bifunctional benefits of PtRu could become muted, or supplanted.

The electrolysis cell was operated in crossover mode (Fig. 2A) so that the methanol in the distillate had to diffuse through the Nafion membrane to reach the anode [24]. This provides some discrimination against larger molecules in the distillate that could poison the anode
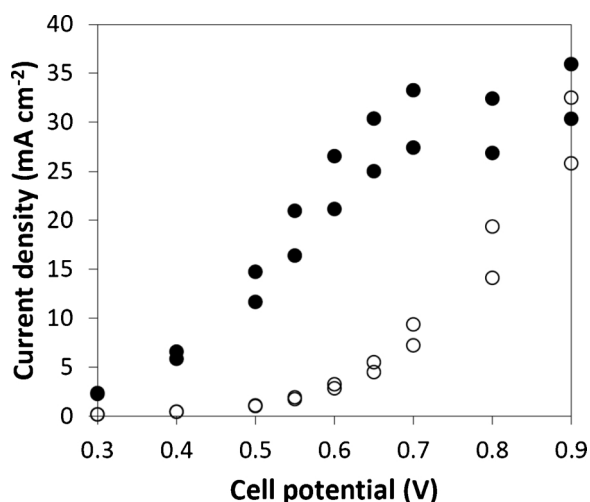
Fig. 4. Polarization curves for oxidation of the softwood oil distillate in a 4-anode cell in crossover mode at Pt black (○) and PtRu black (•) anodes. Data are shown for two electrodes of each type.

catalyst.

The PtRu catalyst oxidized the distillate at much lower potentials than Pt, although currents reached similar values for the two catalysts at 0.9 V. At a cell potential of 0.5 V, the average current density at the two PtRu electrodes was $13\,mA\,cm^{-2}$, and a limiting value of ca. $30\,mA\,cm^{-2}$ was reached at 0.7 V. These results demonstrated that the distillate can be electrolyzed at much lower potentials than water. The current densities obtained with the PtRu catalyst are similar to reported values for electrolysis of various types of biomass in 85% phosphoric acid at 100 °C [16]. In contrast, much higher potentials were required to produce hydrogen at similar current densities from electrolysis of biomass components such as benzyl alcohol and furfural in 1 M NaOH at ambient temperature [15], and microbial electrolysis cells generally produce $< 10\,mA\,cm^{-2}$ at 1.0 V [14].

The current (*I*) measured in the electrolysis cell provides a direct measure of the hydrogen production rate (d*V*/d*t*) via Faraday's law (eq. 3), since there are no other feasible products at the cathode.

$$dV/dt = V_{mol}I/2\,F \qquad (3)$$

where V_{mol} is the molar volume of hydrogen ($24.0\,dm^3\,mol^{-1}$ at 20 °C and 1 bar). This has been well established in a number of previous reports on the electrolysis of organic fuels, including methanol [10,19,30].

Operation of the cell employed here in crossover mode at 80 °C with 1 M methanol produced a limiting current of ca. $250\,mA\,cm^{-2}$ at ca. 0.45 V for PtRu and ca. 0.65 V for Pt (Fig. 5). The much lower currents observed in Fig. 4, for a distillate containing 2.02 M methanol, indicate that there was severe poisoning of both the PtRu and Pt catalysts by other components in the distillate. Consequently, identification and removal of the poisoning species would greatly increase the performance of the cell, and its efficiency for hydrogen production.

3.2. Effects of acetic acid, hydroxyacetone, and acrolein on methanol oxidation

In order to ascertain how the main components (acetic acid, hydroxyacetone, and acrolein) of the softwood oil distillate influenced methanol oxidation, each was added separately to a 1 M methanol solution. Polarization curves (crossover mode) for these mixtures at Pt and PtRu black electrodes are shown in Fig. 5. For 1 M MeOH alone, the limiting current at high potentials was the same at both catalysts because it is controlled by the rate of diffusion of methanol through the cathode and membrane. However, the half-wave potential is much
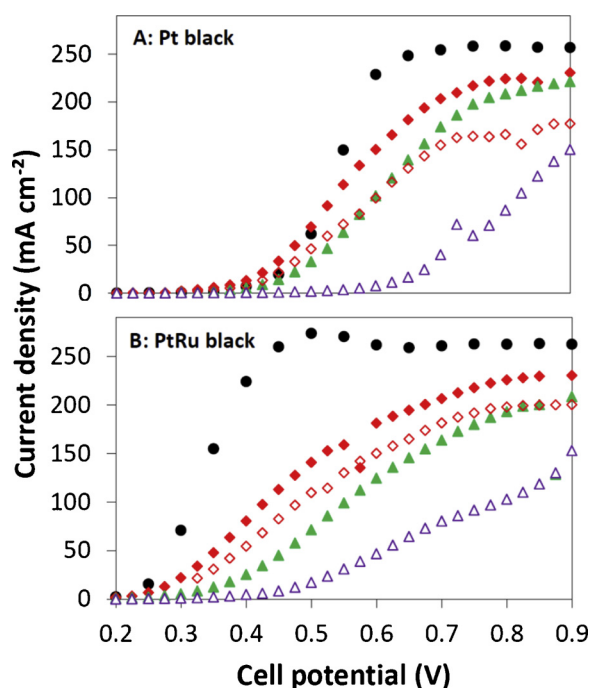

Fig. 5. Polarization curves for oxidation of 1 M MeOH (•), and 1 M MeOH solutions containing 0.1 M acetic acid (♦), 1 M acetic acid (◇), 0.1 M hydroxyacetone (▲), and 0.1 M acrolein (△) at Pt black (A) and PtRu black (B) anodes in a 4-anode cell in crossover mode. Data are averages for two electrodes of each type.

lower for PtRu due to promotion of methanol oxidation by surface Ru−OH groups via the bifunctional effect.

Addition of 0.1 M acetic acid to the methanol solution increased the half-wave potential and decreased the limiting current at both catalysts, indicating that it had a significant poisoning effect, and that the mass-transport limit could no longer be reached. However, the effect was lower at Pt than PtRu. At 0.5 V, where the limiting current was attained at PtRu with 1 M methanol, addition of 0.1 M acetic acid decreased the current ($I_{0.5}$) by 49% at PtRu, but had a negligible effect at Pt. Increasing the acetic acid concentration to 1 M produced a relatively small additional effect at both catalysts, decreasing $I_{0.5}$ by 60% at PtRu and 25% at Pt, relative to methanol alone. Consequently, Pt shows significant tolerance to the high levels of acetic acid in pyrolysis oil distillates, while PtRu is much less tolerant. However, the bifunctional effect of PtRu still allowed it to outperform Pt at all potentials.

The differences here between the Pt and PtRu anode catalysts indicate that the poisoning effects occur primarily at the anode. However, the presence of acetic acid may also increase the overpotential at the cathode, although this is unlikely to be a significant effect because of the much higher inherent rate of the hydrogen evolution reaction relative to methanol oxidation.

The effects of 0.1 M hydroxyacetone were similar to those of 1 M acetic acid, decreasing $I_{0.5}$ by 69% at PtRu and 47% at Pt, relative to methanol alone. However, in this case the better tolerance of the Pt catalyst caused it to outperform PtRu at potentials above 0.6 V. In contrast, 0.1 M acrolein severely poisoned the Pt catalyst, decreasing $I_{0.5}$ by 96%, while PtRu showed slightly better tolerance, with $I_{0.5}$ decreased by 90%. The C═C bond of acrolein allows it to adsorb quite strongly onto Pt (mainly via the carbonyl group) [31], and so it competes strongly with the weak adsorption of methanol. The Ru sites at the surface of the PtRu catalyst limit the number of contiguous Pt sites, which may inhibit acrolein adsorption to some extent.

The differences between the effects of the added impurities on the polarization curves obtained with the Pt vs. PtRu anode catalyst may also be influenced by differences in the faradaic efficiency of methanol

oxidation, due to the formation of formaldehyde and/or formic acid as partial oxidation products [32,33]. Under the conditions employed here, in crossover mode, the faradaic efficiency would be ca. 80% in the absence of impurities [34], but is likely to be significantly lower when Pt sites on the catalyst are occupied by adsorbed impurities.

The results shown in Fig. 5 demonstrate that better separation of methanol from other components of the pyrolysis oil will greatly increase the electrolysis efficiency and current density that can be obtained. The high boiling points (bp) of acetic acid (bp = 118 °C) and acetol (bp = 145 °C) relative to methanol (bp = 65 °C) should allow their concentrations to be decreased by fractional distillation to levels where they will not significantly interfere, while acrolein (bp = 53 °C) presents a more challenging problem.

3.3. Distillates from bark oil

Although effective for upgrading pyrolysis oils and isolation of low molecular weight components, the short-path vacuum distillation described in [23] is a batch process, slow, and difficult to scale up. In addition, the distillate that was produced from the softwood oil contained impurities such as acrolein that severely poison the catalyst in the electrolysis cell. Consequently, distillates for further work were produced by using a conventional laboratory scale fractional distillation. In addition, the aqueous phase of a softwood bark oil was employed as a feedstock, instead of softwood oil. The aquoues phase does not contain the heavier organic species and therefore minimizes the risk of polymerization and other reactions that can occur with use of the whole wood based oil at temperatures greater than 80 °C. There are a number of reactions associated with the heavier organic fraction (e.g. esterification, polymerization, and condensation) predominantly forming oligomers and polymers, that occur as the temperature is increased [35,36].

The bark oil contained much more water than the softwood oil (60–70% vs. ca. 35%), and consequently spontaneously separated into organic and aqueous phases, in a ca. 30:70 vol ratio. The crude aqueous phase is not suitable as a burner fuel, but can be upgraded to meet the ASTM D7544-12 standard by distilling off sufficient water. Here, the water content of a sample was decreased from 62 to 32 mass% with an increase in the (HHV) from < 10 MJ kg^{-1} (incomplete combustion) to 16 MJ kg^{-1}. The methanol-rich distillate can be used in an electrolysis cell to produce hydrogen and as a source of other value-added chemicals.

Table 1 shows the concentrations of the major components of the first four fractions obtained from the aqueous phase of bark oil. The first 5 mL fraction of distillate contained 2.88 M methanol and a relatively low concentration of acetic acid. However, based on the data in Fig. 5, the hydroxyacetone and acrolein levels were too high for it to be used effectively in an electrolysis cell. Consequently, it was diluted to 1 M methanol before electrolysis.

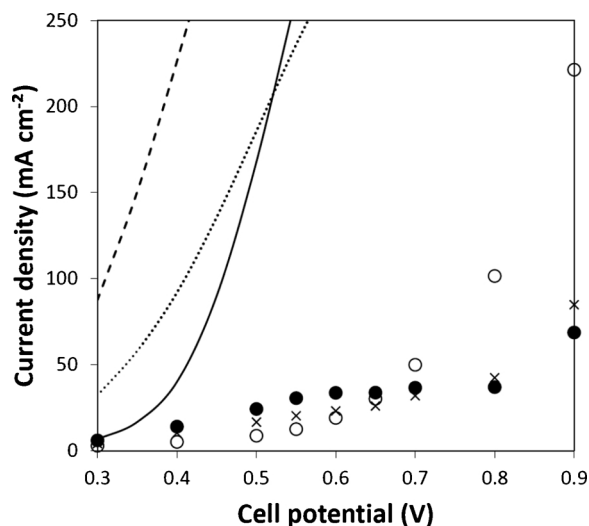Fig. 6 shows polarization curves for the diluted first fraction from

Fig. 6. Polarization curves for oxidation of the bark oil distillate (symbols) and 1 M MeOH (lines) in the 9-anode cell in anode polarization mode at Pt/C (○; —), PtRu/C (●; - - -), and mixed Pt/C + PtRu/C (x; ·····) anodes. Average currents for three electrodes of each type are shown.

the bark oil distillation. A nine-anode cell with three Pt/C anodes, three PtRu/C anodes and three mixed Pt/C + PtRu/C anodes was used in anode polarization mode. Data for electrolysis of 1 M methanol is shown for comparison. Although the bark oil distillate provided much lower currents than methanol alone, the results in Fig. 6 are significant in the context of other studies of biomass electrolysis, as discussed in Section 3.1. Notably, a current of 14 mA cm^{-2} was obtained for the PtRu/C catalyst at 0.4 V, and 220 mA cm^{-2} was obtained for the Pt/C catalyst at 0.9 V, which is ca. 0.6 V lower than the potential required for water electrolysis. Combining the two catalysts did not provide any advantage over the individual Pt/C and PtRu/C catalysts.

The performance of the bark oil distillate seen in Fig. 6 is similar to that seen for the softwood oil distillate at the PtRu catalyst in Fig. 4. However, this was achieved with a single distillation on a 10 times larger scale. Other fractions from the bark oil distillation, listed in Table 1, were not tested directly in an electrolysis cell because they contained too much hydroxyacetone and acrolein relative to methanol.

3.4. Permeates from bark oil

Pervaporation was explored as an alternative method for separating water and other relatively low boiling components from bark oil. It is a membrane separation process in which one or more components from a liquid feed permeate through a membrane and evaporate on the other side. In this case, the condensed vapour stream (permeate) was mainly water, but contained methanol, acetic acid, and a number of other minor components (Table 2). Three different commercial membranes were tested, Nafion 211, Pervap 4155-30, and Pervap 4101. The concentrations of the main components in the permeates are summarized in Table 2. The properties of the residual, enhance oil will be reported elsewhere. The Pervap 4101 membrane provided the best enhanced oil, lowering the water content from 70 to 21 mass% and consequently increasing the heating value from < 10 MJ kg^{-1} to 16 MJ kg^{-1}.

The water selectivity increases with increased crosslinking of the PVA separation layer of the Pervap membranes, and so the permeate obtained with Pervap 4101 contained significantly lower concentrations of organic components than the permeate obtained with Pervap 4155-30. The Nafion membrane produced a permeate with higher concentrations of methanol, acetic acid, and formic acid. Notably, all of the permeates contained lower concentrations of acrolein than the distillates, and the acrolein content of the Pervap 4101 permeate was below the detection limit of the NMR analysis (i.e. < 0.001 M).

Table 1
Concentrations of the main components of the first four distillate fractions obtained from the aqueous phase of bark oil. Fraction 1 was 5 mL, while the others were 10 mL.

Component	Fraction			
	1	2	3	4
[methanol]/M	2.88	1.29	0.92	0.63
[acetic acid]/M	0.23	0.33	0.37	0.38
[hydroxyacetone]/M	0.05	0.13	0.16	0.16
[acrolein]/M	0.07	0.04	0.03	0.03
[formic acid]/M	0.01	0.02	0.03	0.03
[furfural]/M	0.05	0.03	0.03	0.02
[glycolaldehyde]/M	0.000	0.007	0.012	0.015
[isoeugenol]/M	0.002	0.004	0.004	0.006

Table 2

Concentrations of the main components of permeates obtained from the aqueous phase of bark oil.

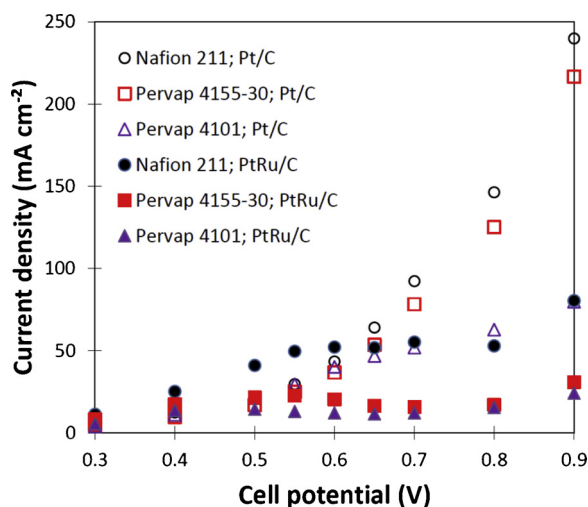| Component	Membrane		
	Nafion 211	Pervap 4155-30	Pervap 4101
[methanol]/M	0.62	0.54	0.14
[acetic acid]/M	1.05	0.47	0.08
[acrolein]/M	0.02	0.02	–
[hydroxyacetone]/M	0.18	0.21	0.04
[formic acid]/M	0.14	0.04	0.02
[furfural]/M	0.017	0.019	–
[glycolaldehyde]/M	0.025	0.033	0.011
[isoeugenol]/M	0.004	0.004	–

– Not detected.

Fig. 7. Polarization curves (average currents for three electrodes) for oxidation of the bark oil permeates in a 9-anode cell in anode polarization mode at Pt/C and PtRu/C anodes. The pervaporation membrane and catalyst are indicated in the legend.

Polarization curves for electrolysis of the permeates at Pt/C and PtRu/C anodes in anode polarization mode are shown in Fig. 7 (data for the mixed Pt/C + PtRu/C anodes are omitted for clarity). As for the bark oil distillate (Fig. 6), the PtRu/C catalyst produced the highest currents at low potentials, while the Pt/C catalyst produced much higher currents at high potentials. The highest current at 0.5 V, obtained with the Nafion 211 permeate, was 41 mA cm^{-2}, which is significantly higher than the 24 mA cm^{-2} obtained with the distillate. At 0.9 V, the Nafion 211 permeate also provided the highest current, 240 mA cm^{-2}, which was slightly higher than the value of 221 mA cm^{-2} obtained with the distillate.

The differences in the performances of the permeates obtained with the Nafion and Pervap membranes can primarily be accounted for by the differences in their methanol contents. The Nafion permeate had the highest methanol concentration and produced the highest currents, while the much lower methanol concentration in the Pervap 4101 permeate produced the lowest currents. However, the performance of the Pervap 4155-30 permeate at the PtRu/C anodes was low relative to its methanol concentration. This cannot be accounted for by either hydroxyacetone, acrolein, furfural, glycolaldehyde, or isoeugenol which were present at similar concentrations to the Nafion permeate, and so must have been due to other impurities that were not be identified in the NMR spectra.

4. Conclusions

Removal of water from pyrolysis oil by distillation or pervaporation, to improve its heating value, produces aqueous solutions containing a potentially valuable mixture of chemicals. Methanol in these solutions can be electrochemically oxidized to produce hydrogen at lower potentials (< 0.5 V) than for water electrolysis (ca. 1.5 V), while preserving acetic acid and other components for further separation. Methanol concentrations as high as 2.9 M and 0.7 M were obtained by fractional distillation and pervaporation, respectively. Electrolysis currents as high as 44 mA cm^{-2} at 0.5 V and 240 mA cm^{-2} at 0.9 V were obtained. However, these are significantly lower than those obtained with pure aqueous methanol due to poisoning of the electrocatalysts by acetic acid, hydroxyacetone, acrolein, and other impurities. Consequently, there is scope for substantial improvements through scale-up, and optimization of the separation processes.

References

[1] B. Emonts, S. Schiebahn, K. Gorner, D. Lindenberger, P. Markewitz, F. Merten, D. Stolten, Re-energizing energy supply: electrolytically-produced hydrogen as a flexible energy storage medium and fuel for road transport, J. Power Sources 342 (2017) 320–326.

[2] A. Buttler, H. Spliethoff, Current status of water electrolysis for energy storage, grid balancing and sector coupling via power-to-gas and power-to-liquids: a review, Renew. Sustain. Energy Rev. 82 (2018) 2440–2454.

[3] K. Alanne, S.L. Cao, Zero-energy hydrogen economy (ZEH(2)E) for buildings and communities including personal mobility, Renew. Sustain. Energy Rev. 71 (2017) 697–711.

[4] B. You, Y.J. Sun, Innovative strategies for electrocatalytic water splitting, Acc. Chem. Res. 51 (2018) 1571–1580.

[5] C. Coutanceau, S. Baranton, Electrochemical conversion of alcohols for hydrogen production: a short overview, Wiley Interdisc. Rev.-Energy Environ. 5 (2016) 388–400.

[6] B. You, X. Liu, X. Liu, Y.J. Sun, Efficient H$_2$ evolution coupled with oxidative refining of alcohols via a hierarchically porous nickel bifunctional electrocatalyst, ACS Catal. 7 (2017) 4564–4570.

[7] B. You, N. Jiang, X. Liu, Y.J. Sun, Simultaneous H$_2$ generation and biomass upgrading in water by an efficient noble-metal-free bifunctional electrocatalyst, Angew. Chem. Int. Ed. 55 (2016) 9913–9917.

[8] N. Jiang, B. You, R. Boonstra, I.M.T. Rodriguez, Y.J. Sun, Integrating electrocatalytic 5-hydroxymethylfurfural oxidation and hydrogen production via Co-P-derived electrocatalysts, ACS Energy Lett. 1 (2016) 386–390.

[9] Y.X. Chen, A. Lavacchi, H.A. Miller, M. Bevilacqua, J. Filippi, M. Innocenti, A. Marchionni, W. Oberhauser, L. Wang, F. Vizza, Nanotechnology makes biomass electrolysis more energy efficient than water electrolysis, Nat. Commun. 5 (2014).

[10] B. Guenot, M. Cretin, C. Lamy, Clean hydrogen generation from the electrocatalytic oxidation of methanol inside a proton exchange membrane electrolysis cell (PEMEC): effect of methanol concentration and working temperature, J. Appl. Electrochem. 45 (2015) 973–981.

[11] V. Bambagioni, M. Bevilacqua, C. Bianchini, J. Filippi, A. Lavacchi, A. Marchionni, F. Vizza, P.K. Shen, Self-sustainable production of hydrogen, chemicals, and energy from renewable alcohols by electrocatalysis, ChemSusChem 3 (2010) 851–855.

[12] E.O. Kilic, A.S. Koparal, U.B. Ogutveren, Hydrogen production by electrochemical decomposition of formic acid via solid polymer electrolyte, Fuel Process. Technol. 90 (2009) 158–163.

[13] A.P. Borole, Sustainable and efficient pathways for bioenergy recovery from low-value process streams via bioelectrochemical systems in biorefineries, Sustainability 7 (2015) 11713–11726.

[14] L. Lu, Z.Y.J. Ren, Microbial electrolysis cells for waste biorefinery: a state of the art review, Bioresour. Technol. 215 (2016) 254–264.

[15] B. You, X. Liu, N. Jiang, Y.J. Sun, A general strategy for decoupled hydrogen production from water splitting by integrating oxidative biomass valorization, J. Am. Chem. Soc. 138 (2016) 13639–13646.

[16] T. Hibino, K. Kobayashi, M. Ito, O. Ma, M. Nagao, M. Fukui, S. Teranishi, Efficient hydrogen production by direct electrolysis of waste biomass at intermediate temperatures, ACS Sustain. Chem. Eng. 6 (2018) 9360–9368.

[17] T. Hibino, K. Kobayashi, M. Ito, M. Nagao, M. Fukui, S. Teranishi, Direct electrolysis of waste newspaper for sustainable hydrogen production: an oxygen-functionalized porous carbon anode, Appl. Catal. B Environ. 231 (2018) 191–199.

[18] M. Simoes, S. Baranton, C. Coutanceau, Electrochemical valorisation of glycerol,

Chemsuschem 5 (2012) 2106–2124.

[19] A.R. de la Osa, A.B. Calcerrada, J.L. Valverdea, E.A. Baranova, A. de Lucas-Consuegra, Electrochemical reforming of alcohols on nanostructured platinum-tin catalyst-electrodes, Appl. Catal. B Env. 179 (2015) 276–284.

[20] H. Li, Z. Fang, R.L. Smith, S. Yang, Efficient valorization of biomass to biofuels with bifunctional solid catalytic materials, Prog. Energy Combust. Sci. 55 (2016) 98–194.

[21] H.J. Kim, Y. Kim, D.E. Lee, J.R. Kim, H.J. Chae, S.Y. Jeong, B.S. Kim, J. Lee, G.W. Huber, J. Byun, S. Kim, J. Han, Coproducing value-added chemicals and hydrogen with electrocatalytic glycerol oxidation technology: experimental and techno-economic investigations, ACS Sustain. Chem. Eng. 5 (2017) 6626–6634.

[22] L. Du, Y.Y. Shao, J.M. Sun, G.P. Yin, C.Y. Du, Y. Wang, Electrocatalytic valorisation of biomass derived chemicals, Catal. Sci. Technol. 8 (2018) 3216–3232.

[23] S. Rahman, R. Helleur, S. MacQuarrie, S. Papari, K. Hawboldt, Upgrading and isolation of low molecular weight compounds from bark and softwood bio-oils through vacuum distillation, Sep. Purif. Technol. 194 (2018) 123–129.

[24] T.M. Brueckner, P.G. Pickup, Kinetics and stoichiometry of methanol and ethanol oxidation in multi-anode proton exchange membrane cells, J. Electrochem. Soc. 64 (2017) F1172–F1178.

[25] S. Papari, K. Hawboldt, R. Helleur, Production and characterization of pyrolysis oil from sawmill residues in an auger reactor, Ind. Eng. Chem. Res. 56 (2017) 1920–1925.

[26] R.M. Altarawneh, P.G. Pickup, Product distributions and efficiencies for ethanol oxidation in a proton exchange membrane electrolysis cell, J. Electrochem. Soc. 164 (2017) F861–F865.

[27] Y.V. Tolmachev, O.A. Petrii, Pt-Ru electrocatalysts for fuel cells: developments in the last decade, J. Solid State Electrochem. 21 (2017) 613–639.

[28] A.S. Moura, J.L.C. Fajin, M. Mandado, M. Cordeiro, Ruthenium-platinum catalysts and direct methanol fuel cells (DMFC): a review of theoretical and experimental breakthroughs, Catalysts 7 (2017) 47.

[29] D. Chu, S. Gilman, Methanol electro-oxidation on unsupported Pt-Ru alloys at different temperatures, J. Electrochem. Soc. 143 (1996) 1685–1690.

[30] C. Lamy, T. Jaubert, S. Baranton, C. Coutanceau, Clean hydrogen generation through the electrocatalytic oxidation of ethanol in a proton exchange membrane electrolysis cell (PEMEC): effect of the nature and structure of the catalytic anode, J. Power Sources 245 (2014) 927–936.

[31] J.C. de Jesus, F. Zaera, Adsorption and thermal chemistry of acrolein and crotonaldehyde on Pt(111) surfaces, Surf. Sci. 430 (1999) 99–115.

[32] H.S. Wang, C. Wingender, H. Baltruschat, M. Lopez, M.T. Reetz, Methanol oxidation on Pt, PtRu, and colloidal Pt electrocatalysts: a DEMS study of product formation, J. Electroanal. Chem. 509 (2001) 163–169.

[33] M. Chojak-Halseid, Z. Jusys, R.J. Behm, Methanol oxidation over a Pt/C catalyst at high temperatures and pressure: an online electrochemical mass spectrometry study, J. Phys. Chem. C 114 (2010) 22573–22581.

[34] P. Majidi, R.M. Altarawneh, N.D.W. Ryan, P.G. Pickup, Determination of the efficiency of methanol oxidation in a direct methanol fuel cell, Electrochim. Acta 199 (2016) 210–217.

[35] A. Oasmaa, I. Fonts, M.R. Pelaez-Samaniego, M.E. Garcia-Perez, M. Garcia-Perez, Pyrolysis oil multiphase behavior and phase stability: a review, Energy Fuels 30 (2016) 6179–6200.

[36] E. Alsbou, R. Helleur, Whole sample analysis of bio-oils and thermal cracking fractions by Py-GC/MS and TLC-FID, J. Anal. Appl. Pyrolysis 101 (2013) 222–231.